What Is the Distance to the Wall in Lattice Simulations?

3 AUTHORS:

Iwao Teraoka
Polytechnic Institute of New York University
113 PUBLICATIONS **2,887** CITATIONS

SEE PROFILE

Peter Cifra
Slovak Academy of Sciences
96 PUBLICATIONS **1,027** CITATIONS

SEE PROFILE

Yongmei Wang
The University of Memphis
91 PUBLICATIONS **1,455** CITATIONS

SEE PROFILE

What Is the Distance to the Wall in Lattice Simulations?

Iwao Teraoka,*,† **Peter Cifra,**‡ **and Yongmei Wang**§

Herman F. Mark Polymer Research Institute, Polytechnic University, 333 Jay Street, Brooklyn, New York 11201; Polymer Institute, Slovak Academy of Sciences, Dúbravská cesta 9, 842 36 Bratislava, Slovak Republic; and Department of Chemistry, North Carolina A&T State University, Greensboro, North Carolina 27411

ABSTRACT: Lattice Monte Carlo simulations are widely used to study the effect of walls on the concentration profile in polymer solutions. The scaling theory predicts that the monomer density at a distance x from the wall, reduced by the bulk density, is proportional to $(x/R_{g0})^{1/\nu}$ at low concentrations, and the correlation length replaces R_{g0} in the semidilute solution, where R_{g0} is the radius of gyration and ν is the Flory exponent for the chain dimension. We conducted simulations for long chains on a cubic lattice to find that a positive penetration depth γ is needed to see an agreement with the theory. The monomers perceive a theoretical wall at an off-lattice position of γ behind the presumed wall on the lattice points. We found $\gamma \sim 0.13$ of the lattice unit at low concentrations but ~ 0.36 in the semidilute solution for athermal chains. For Θ solutions, γ was $0.31-0.36$ at all concentrations. We ascribe the positive γ to uneven chain segment propagation in the chain update in a nonuniform density profile.

Introduction

Impenetrable walls are frequently used in lattice simulations to study how the polymer chains change their properties when placed near the wall or confined to a slit.[1−15] The depletion of the monomer density near the wall is one of the typical phenomena. To compare the simulation results with theories formulated in a continuous space for a polymer chain model of a flexible thin thread, we superimpose a continuous coordinate system onto the cubic lattice. In this paper, we consider how to define the theoretical distance to the wall in the superimposed continuum.

We could decrease the ambiguity by employing a larger simulation box and longer chains. It would require, however, a longer machine time and a greater memory size by many orders of magnitude to carry out simulations for the same volume fraction of the polymer and the same chain dimension relative to the slit width. It is always desirable to make sense of the simulation data down to one lattice unit.

The scaling theory[16] predicts the density profile of a dilute polymer solution in contact with a solid wall. The density $\phi(x)$ at distance x from the wall, reduced by the bulk density ϕ_{bulk}, is a universal function f of x/R_{g0}, where R_{g0} is the radius of gyration in the dilute unconfined solution. The function f should satisfy

$$f(z) = \begin{cases} 1 & (z \to \infty) \\ \sim z^m & (z \ll 1) \end{cases} \tag{1}$$

where the exponent $m = 1/\nu$ is 5/3 or $1/0.59 = 1.69$ for athermal chains and 2 for Θ chains. For the ideal chains, $m = 2$ agrees with the exact result obtained by Casassa[17] for a Gaussian chain. The same result was obtained in the ϵ expansion,[18] where ϵ denotes the difference in the dimension from 4.

In the semidilute solution, the correlation length ξ should replace R_{g0}, but otherwise the same scaling law

† Polytechnic University.
‡ Slovak Academy of Sciences.
§ North Carolina A&T State University.

should hold for $\phi(x)$.[16] Thus, the depletion layer becomes thinner with an increasing concentration. Shih et al.[19] studied the profile of the semidilute solution using the lattice simulations. They found that the simulation results at small x/ξ show a substantial deviation from $(x/\xi)^{5/3}$. To compensate for this disagreement, they assumed $\phi(x)/\phi_{bulk} = 1 - \exp(-\alpha(x/\xi)^m)$ with α being a constant and plotted $\ln(1 - \phi(x)/\phi_{bulk})$ as a function of x/ξ. Interestingly, they recovered $m \cong 5/3$, but the body of the data used for the fitting did not satisfy the condition of $x/\xi \ll 1$. Dickman[20] attempted a similar plot for his simulation results on two-dimensional lattice chains in the Θ condition. He found a substantial deviation from the scaling exponent.

Let us consider a cubic lattice (unit length $= a$) in a simulation box that consists of L_x, L_y, and L_z lattice points in x, y, and z directions, respectively. The periodic boundary condition is imposed in the y and z directions. Monomers can be on any layers from $x = a$ to $x = aL_x$ but are not allowed to step out. Then, we usually think that two parallel walls exist at $x = 0$ and $x = a(L_x + 1)$. In the superimposed continuum, however, the condition that the walls be on the lattice points is lifted. The wall at $x = 0$ can now be anywhere between $x = -a/2$ and $a/2$, because any wall in that range is equally effective in preventing monomers of diameter a from occupying the lattice sites on $x = 0$. We let $x + \gamma$ be the distance to the wall with a penetration depth γ in the range of $|\gamma| \le a/2$, when we consider the monomer density profile near the wall at $x = 0$. Then, $\phi(x)/\phi_{bulk} = f_d((x + \gamma)/R_{g0})$ in dilute solutions and $\phi(x)/\phi_{bulk} = f_{sd}((x + \gamma)/\xi)$ in semidilute solutions, if the slit is sufficiently wide for $\phi(x)$ to have a plateau in the middle of the slit as ϕ_{bulk} (weak confinement). In a narrow slit, $\phi(x)$ does not have a plateau (strong confinement). There is no universal function, but $\phi(x) \sim (x + \gamma)^{1/\nu}$ still holds.[21] Note that the functional forms, f_d and f_{sd}, may be different for the two concentration regimes.

Recently, a couple of Monte Carlo simulation studies[21,22] were conducted to obtain the density profile of a single long chain trapped between two parallel walls. One[22] used self-avoiding walks of $N = 200-8000$ steps

Table 1. Characteristics of Chains Used in Simulations

solvent	N	R_{g0}/a	ϕ^*
athermal	400	14.73	0.0425
	600	18.77	0.0311
	800	22.25	0.0250
	1000	25.52	0.0208
	1400	30.88	0.0165
	2000	37.72	0.0130
theta	1000	17.52	0.0635
	2000	24.81	0.0452
ideal	2000	18.25	

on a cubic lattice. In the study, the density profile near the wall was found to follow the scaling law with respect to x, when a positive γ was added to x. The value of γ/a was 0.3 for $N = 8000$ but smaller for shorter chains. A similar correction to x was introduced in the off-lattice simulation study[21] for a bead−spring model of N beads with a finitely extensible nonlinear elastic potential for connecting bonds and exclusion between nonbonded beads. For the chains with $N = 32-512$, use of $\gamma/a \cong 0.35$ reproduced the scaling relationship between ϕ and x, where a is the maximal extension between the bead centers. These studies demonstrated a need for a positive γ. The master curve, eq 1, has not been obtained in either study, however; the authors did not attempt to obtain a master curve or were interested in profiles only in slits too narrow to have ϕ_{bulk} in the middle of the slit.

We recently conducted a lattice Monte Carlo simulation study on the thermodynamics of chain molecules in the Θ condition equilibrated with a slit.[12] The partition coefficient K_0 in the dilute solution limit followed a power law of $-\ln K_0 \sim (2R_{g0}/d)^{1.714}$, where $d = a(L_x + 1)$ is the slit width without correction. The exponent should be 2 according to the scaling theory, however. Adding a positive $2\gamma \cong 0.8a$ to d solves the problem.

Below we will show that (1) the density profile of ideal chains needs no correction, (2) the density profile of athermal chains at low concentrations obtained for different chain lengths fall on a master curve when $\gamma/a \cong 0.13$ is added, (3) a similar scaling law is observed in semidilute solutions with $\gamma/a \cong 0.36$, and (4) the correct scaling exponent of $m = 2$ is observed for dilute and semidilute solutions in the Θ condition with $\gamma/a = 0.31-0.36$.

Simulation Procedures

Polymer chains consisting of N monomers ($N = 400$, 600, 800, 1000, 1400, 2000) were generated in the simulation box of $L_y = L_z = 256$ for athermal chains and $L_y = L_z = 100$ for Θ and ideal chains. Table 1 lists the chains used in the simulations. Athermal chains were generated as a self-avoiding walk with no interactions between monomers except for the excluded volume. Θ chains were generated as a self-avoiding walk with negative contact energy ($-0.2693k_BT$, where k_BT is the thermal energy) between nonbonded monomers to obtain a zero second virial coefficient.[23] In ideal chains, monomer overlap was allowed, and no interactions were assumed between the monomer and the wall except for no occupancy rule at the walls. Table 1 also lists R_{g0} and the overlap volume fraction ϕ^* in the unconfined solution. We define ϕ^* by $\phi^*[2^{1/2}(R_{g0}/a + \alpha)]^3 = N$. The extra constant α on R_{g0}/a is needed to translate the volume occupied by the chain on the lattice into the one in continuum.[10] It is 0.199 for athermal chains[10] and 0.204 for Θ chains.[12]
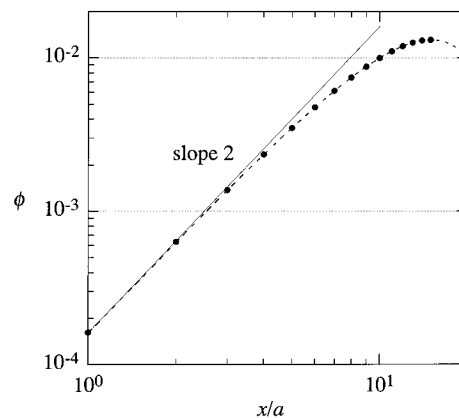

Figure 1. Monomer density profile ϕ of ideal chains in the slit of $L_x = 29$, plotted as a function of x/a. The exact formula for a Gaussian chain with the same radius of gyration is shown by a dashed line. The solid line has a slope of 2.

The Metropolis rule[24] and reptation moves had equilibrated the system before sampling of the monomer density profile started. As many as 4×10^9 trial moves were required for a smooth and symmetric density profile. The average monomer density was calculated for every L_x in the box. What will be shown as the density is the mean of the densities at x and $a(L_x + 1) - x$, unless otherwise specified.

Results

Ideal Chains. The monomer density profile of ideal chains near the walls follows $\sim x^2$ behavior without any correction ($\gamma = 0$). Symbols in Figure 1 show the results for $N = 2000$ in a box of $L_x = 29$. The exact result for a Gaussian chain with the same radius of gyration is shown as a dashed line. It is calculated as[16,25]

$$\frac{\phi(x)}{\phi_{AV}} = \sum_{k,l:odd} \frac{2e_{kl}}{kl} \sin\frac{k\pi x}{d} \sin\frac{l\pi x}{d} \bigg/ \sum_{k:odd} \frac{e_{kk}}{k^2} \quad (2)$$

where $d = a(L_x + 1)$ is the slit width, ϕ_{AV} is the average density in the slit, and

$$e_{kl} = \begin{cases} \dfrac{\exp(-N\epsilon_l) - \exp(-N\epsilon_k)}{N(\epsilon_k - \epsilon_l)} & (k \neq l) \\ \exp(-N\epsilon_k) & (k = l) \end{cases} \quad (3)$$

with $\epsilon_k = (k\pi/d)^2/6$ ($k = 1, 2, ...$). The first term dominates in the sums in the strong confinement limit, and the exact formula becomes a squared sine, $\sin^2(\pi x/d)$. The simulation results are on the theoretical curve, without any need of a correction to x. The asymptote, shown as a solid line, has a slope of 2.

Dilute Athermal Solutions. A sufficiently wide slit of $L_x \geq 5R_{g0}/a$ was used to have a plateau in $\phi(x)$ in the middle of the slit as ϕ_{bulk}. The average monomer density ϕ_{AV} in the slit (= (total number of monomers)/($L_xL_yL_z$)) was around $\phi^*/20$. Figure 2 shows the reduced density $\phi(x)/\phi_{bulk}$ as a function of x/R_{g0} for five lengths of the chains. It does not appear reasonable to draw a master curve with whatever exponent for the data points at $x/R_{g0} < 0.2$, since the data points for different chain lengths spread out. Furthermore, these points are not along the straight line with a slope of 1.69. We consider that the spread is due to the assumption of $\gamma = 0$. With a correction, the profile near the wall should follow the scaling relationship (eq 1): $(x + \gamma)/a \cong (R_{g0}/a)(\phi(x)/$
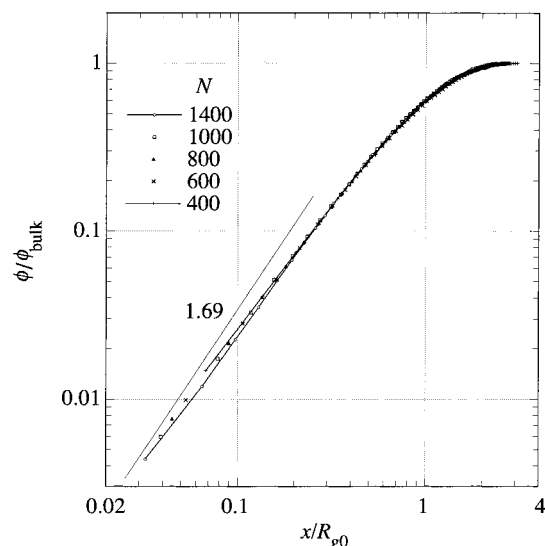
Figure 2. Reduced monomer density profile $\phi(x)/\phi_{bulk}$ of athermal chains at low concentrations, plotted as a function of x/R_{g0} for $N = 1400, 1000, 800, 600,$ and 400. The data for $N = 1400$ and 400 are connected by solid lines. The straight line has a slope of 1.69.
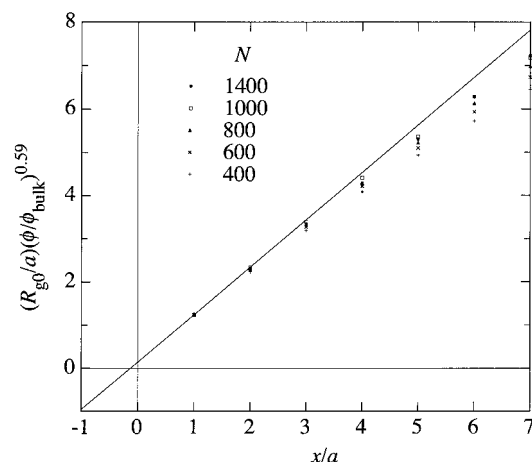

Figure 3. Plot of $(R_{g0}/a)(\phi(x)/\phi_{bulk})^{0.59}$ as a function of x/a for athermal chains at low concentrations. The x-intercept of the straight line gives $-\gamma/a$.

$\phi_{bulk})^{0.59}$. To find the optimal γ/a, we plot $(R_{g0}/a)(\phi(x)/\phi_{bulk})^{0.59}$ as a function of x/a in Figure 3. At small x/a, the data obtained for different values of N fall onto the straight line in the figure, indicating that eq 1 gives a universal function when a positive γ is allowed. The straight line does not pass through the origin. From the intercept on the abscissa, we estimate γ/a to be 0.13. Our penetration depth is smaller than the one obtained by de Joannis et al.[22]

Figure 4 shows the revised plot of $\phi(x)/\phi_{bulk}$ as a function of $(x + \gamma)/R_{g0}$ with $\gamma/a = 0.13$. In this plot, it is justifiable to draw a master curve in the entire range of x/R_{g0}. The master curve is approximated by

$$\frac{\phi(x)}{\phi_{bulk}} = \frac{1 - \exp(-p_1 X)}{1 + p_2 \exp(-p_3 X)} \qquad (4)$$

where $X = [(x + 0.13a)/R_{g0}]^{1.69}$. The optimal fitting parameters were $p_1 = 3.446$, $p_2 = 2.111$, and $p_3 = 1.191$. The master curve assumes the slope of 1.69 at $X \ll 1$.

We conducted simulations for shorter chains ($N = 300, 200, 150,$ and 100) as well, but we could not find
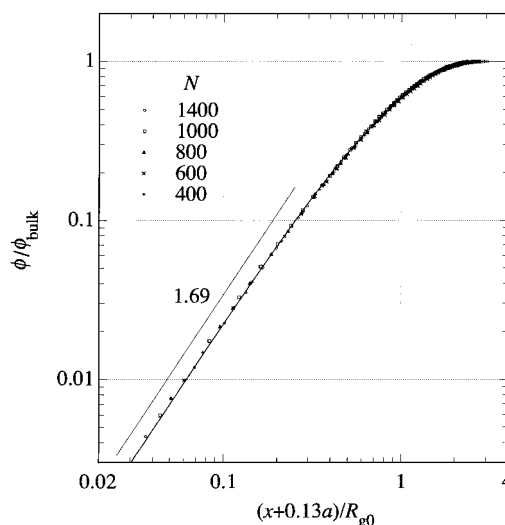

Figure 4. Reduced monomer density profile $\phi(x)/\phi_{bulk}$ of athermal chains at low concentrations, plotted as a function of $(x + 0.36a)/R_{g0}$. The straight line has a slope of 1.69. The solid curve is the optimal fitting by a function that satisfies two theoretical asymptotes.

the appropriate γ/a in a plot similar to Figure 3 with only one layer in the range of $x/R_{g0} < 0.2$. The data lie, however, on the same master curve when the same γ/a is used (not shown).

Semidilute Athermal Solutions. Simulations for semidilute solutions of athermal chains were conducted in narrower slits of $L_x = 30$ and 20 for $N = 2000$ and 1000, respectively. The average density ϕ_{AV} within the slit reduced by ϕ^* was between 4.7 and 8.6 for $N = 2000$ and between 4.4 and 7.7 for $N = 1000$. Static light scattering studies[27] indicate that these concentrations are sufficiently high to allow us to estimate the correlation length in the bulk solution by $\xi = R_{g0}(\phi_{bulk}/\phi^*)^{-\nu/(3\nu-1)}$, where $\nu/(3\nu - 1) = -0.766$. There was a well-defined plateau in the density profile in each of the simulation results, which we used for ϕ_{bulk}; ξ/a for these concentrations is expected to be less than 9.25 for $N = 2000$ and 6.67 for $N = 1000$. It means that the effective confinement was weak at these concentrations. At lower concentrations, we could not see a plateau in the density profile.

Figure 5 displays the reduced density for $N = 2000$ as a function of x/ξ at different values of ϕ_{AV}. Without the correction, data obtained at one of the concentrations are systematically deviated from the other sets of data. It is impossible to draw a master curve that approaches a straight line with a slope of 1.69 in the small x/a limit. Again, we expect that adding γ to x will rectify the problem. To find the optimal γ/a, we plot $(\xi/a)(\phi(x)/\phi_{bulk})^{0.59}$ as a function of x/a in Figure 6. The range of x/a in which $(\xi/a)(\phi(x)/\phi_{bulk})^{0.59}$ is linear to x/a is narrow because of small ξ, especially at high concentrations. Although finding γ/a is not as easy as it is at low concentrations, it appears that $\gamma/a = 0.36$ shown by a straight line is appropriate for the semidilute solutions. As an alternative, we tried different values of γ/a in the double-logarithmic plot of $\phi(x)/\phi_{bulk}$ vs $(x + \gamma)/\xi$ to find that $\gamma/a = 0.36$ gives the optimal overlapping of the data with each other, and they follow the scaling exponent of 1.69 when $x/\xi \ll 1$.

In Figure 7, we show the same data of $\phi(x)/\phi_{bulk}$ but as a function of $(x + 0.36a)/\xi$. All the data are on a master curve. Figure 8 shows the data compiled from

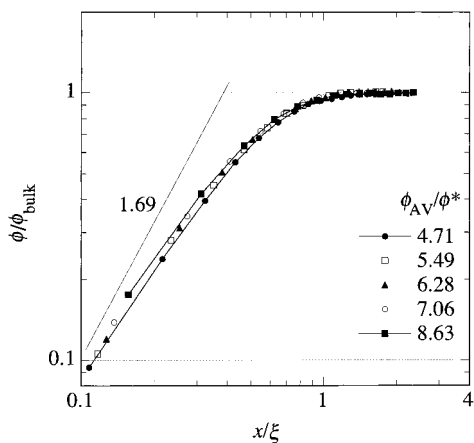**Figure 5.** Reduced monomer density $\phi(x)/\phi_{\text{bulk}}$ of athermal chains of $N = 2000$ in semidilute solutions, plotted as a function of x/ξ for $\phi_{\text{AV}}/\phi^* = 4.71$, 5.49, 6.28, 7.06, and 8.63. The data for $\phi_{\text{AV}}/\phi^* = 4.71$ and 8.63 are connected by solid lines. The straight line has a slope of 1.69.
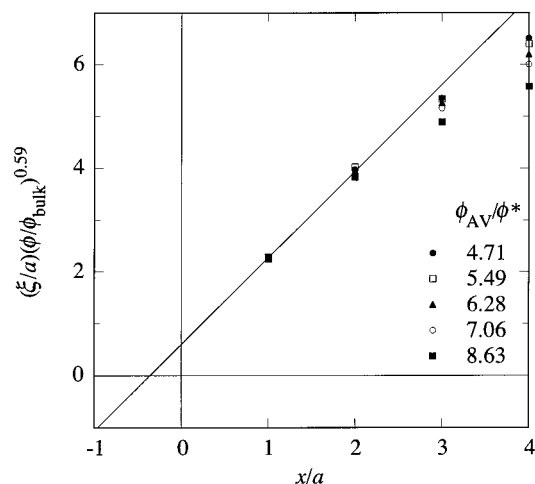

Figure 6. Plot of $(\xi/a)(\phi(x)/\phi_{\text{bulk}})^{0.59}$ as a function of x/a for athermal chains in semidilute solutions. The x-intercept of the straight line gives $-\gamma/a$.
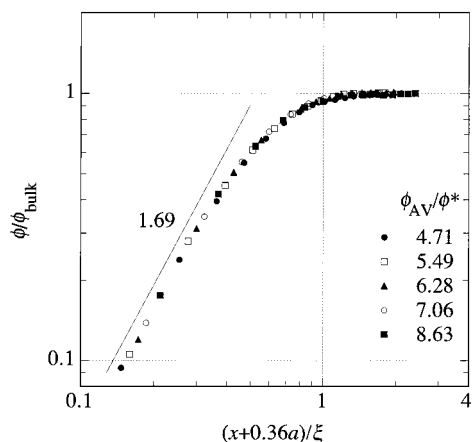

Figure 7. Reduced monomer density profile $\phi(x)/\phi_{\text{bulk}}$ for athermal chains with $N = 2000$ plotted as a function of $(x + 0.36a)/\xi$. The straight line has a slope of 1.69.

different concentrations for $N = 2000$, $L_x = 30$ and $N = 1000$, $L_x = 20$. Data for the two lengths are on a single master curve. Comparison of Figures 4 and 8 indicates that the $\phi(x)/\phi_{\text{bulk}}$ data obtained in different concentration ranges do not overlap. The two universal functions obtained for the two concentration ranges are different.
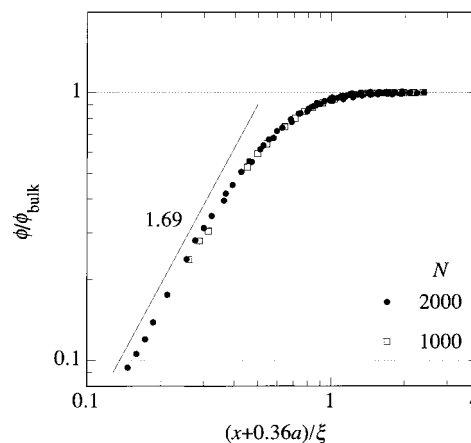

Figure 8. Reduced monomer density $\phi(x)/\phi_{\text{bulk}}$ of athermal chains with $N = 2000$ and 1000 in the semidilute solution, plotted as a function of $(x + 0.36a)/\xi$ for two different chain lengths N. The straight line has a slope of 1.69.

In fact, we failed to fit the semidilute solution data in Figure 8 by eq 4.

Θ Solutions. The density profiles were obtained for Θ chains with $N = 2000$ and 1000 in a simulation box of $L_x = 29$ and 49 at different concentrations. The slit was not sufficiently wide to have a plateau in the density profile except for $N = 1000$ at the highest concentration. In athermal chains, in contrast, strong repulsions between chains force monomers to spread toward the walls at $\phi_{\text{AV}} > \phi^*$, as we have seen in Figure 5. In the Θ chains, the density profile remains centered at the middle of the slit because of compensating repulsive and attractive interactions between monomers (near-zero second virial coefficient). The tendency for the Θ chains to form dynamic clusters makes the profile more protrusive at the slit center. The lack of plateau forces us to abandon the master curve. Nevertheless, it is possible to estimate the penetration depth γ/a by plotting $[\phi(x)]^\nu = [\phi(x)]^{1/2}$ as a function of x/a. The result was $\gamma/a = 0.31-0.33$ at $\phi_{\text{AV}} < \phi^*$ but increases to ~ 0.36 in the semidilute solutions, common to $N = 1000$ and 2000. Parts a and b of Figure 9 show $\phi(x)$ as a function of $x/a + 0.36$. The straight lines have a slope of 2. All the plots follow asymptotically the straight lines when x/a is sufficiently small. Without the correction, there is a large deviation from the scaling exponent of 2 (not shown).

To compare the density profile of a Θ chain with the exact formula for a Gaussian chain given by eq 2, we compare the density profile of a strongly confined chain ($N = 1000$ in a slit of $L_x = 11$) in Figure 10. The dashed line represents eq 2 without correction and the solid line with a correction of $\gamma/a = 0.36$. The curve with the correction fits the simulation data much better than the other curve does. The profile of a Θ chain in the slit follows closely that of a Gaussian chain with the same dimension.

Discussion

A positive penetration depth γ is needed for the density profile obtained in lattice simulations to agree with the prediction of the scaling theory in dilute solutions as well as in semidilute solutions. The need is not to compensate a mismatch between the continuum and the discrete space, since $\gamma = 0$ in ideal chains on the discrete lattice. The fact that there is no need for γ for ideal chains but there is one for a positive
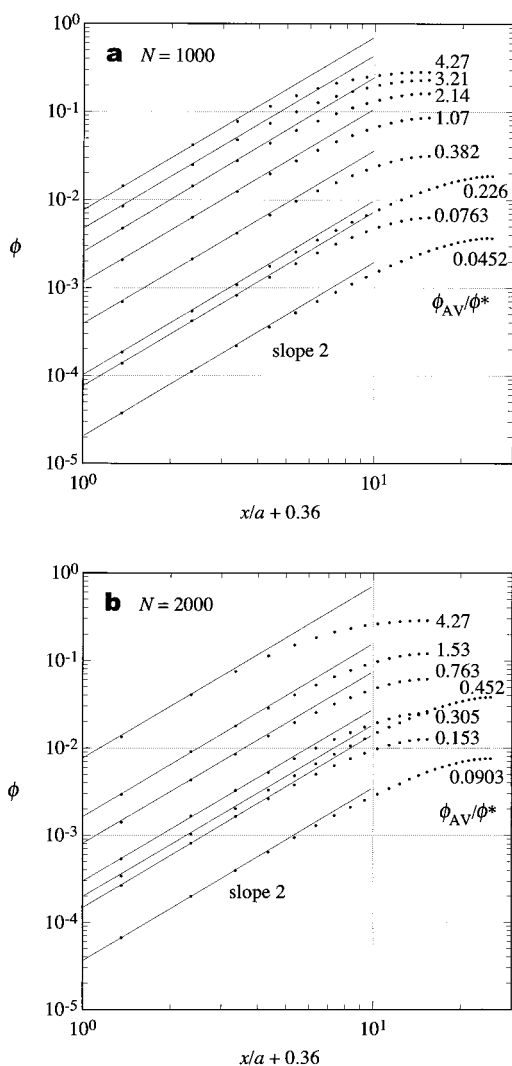
Figure 9. Monomer density profile ϕ of Θ chains of in the slit of $L_x = 29$ and 49 at different concentrations, plotted as a function of $x/a + 0.36$. The straight lines have a slope of 2. (a) $N = 1000$, (b) $N = 2000$.
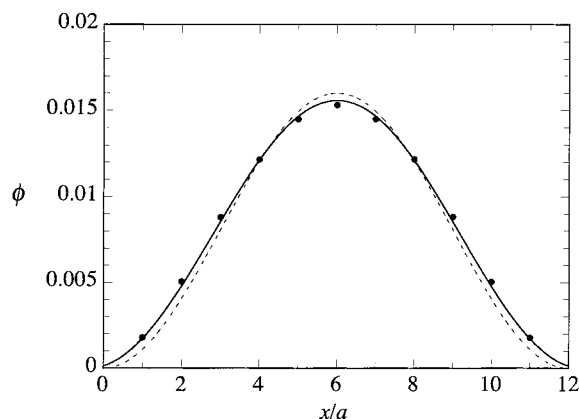

Figure 10. Monomer density profile ϕ of a Θ chain with $N = 1000$ across a slit of width $L_x = 11$. The profile for a Gaussian chain with the same radius of gyration is also shown. The dashed line is without correction, and the solid line is with a correction of $\gamma/a = 0.36$.

γ for athermal and Θ chains indicates that this correction is related to the volume occupancy in the layers near the walls. The optimal penetration depth appears to depend on the concentration and the effective confinement strength. The latter can be conveniently

Table 2. Optimal Penetration Depth Reduced by the Lattice Unit

	weak confinement	strong confinement
athermal, dilute	0.13	(0.3)[a]
athermal, semidilute	0.36	
Θ, dilute		0.31−0.33
Θ, semidilute	0.36	

[a] From de Joannis et al.[22]

measured by the presence of a plateau in the density profile, not by the ratio of R_{g0} to the slit width, as the length of the coherently moving units sensed by the slit for the partitioning, changes from R_{g0} to ξ with an increasing concentration.[9] We tabulate the optimal γ/a in Table 2. We include the estimate obtained by de Joannis et al.[22] in their cubic lattice simulations for a single chain of $N = 8000$. Our estimates of γ/a for dilute solutions are comparable to that estimate. The penetration is universal, regardless of the concentration range or the confinement strength, although it is shallow at low concentrations in a weak confinement. It is now apparent that the discrepancy observed in the lattice simulations for the density profile of confined semidilute solutions[19,20] is due to a neglect of the positive penetration depth. We can ascribe the discrepancy in the partition coefficient of the Θ chains at low concentrations[12] to the same neglect.

We refrain from comparing our penetration depth with the one estimated in the off-lattice Monte Carlo simulations.[21] The difference in the bonded contact and nonbonded contact interactions between the two simulation methods and the difference in the definition of the distance to the wall preclude the comparison at this moment. Further off-lattice simulation studies are needed.

The need for a positive γ/a indicates that the monomer density is higher in layers next to the walls and in nearby layers than it is predicted by the scaling prediction. There is an incentive for the chain to spread to the walls, especially at high concentrations or in the strong confinement. One of the possible hypotheses to explain the incentive is as follows. In the reptation move, the chain is allowed to move when one of its ends, selected randomly, tries to move into an unoccupied site. Otherwise, it does not move. We pay attention to the monomer density in the first layer. The site occupancy in the first layer decreases when the chain end in that layer moves away to the second layer. The occupancy increases when the chain end in the second layer moves into the first layer. The decrease occurs when the other end of the chain, located somewhere away from the wall, tries to move into an unoccupied site. The probability of a successful move is proportional to $1 - \phi_{TOE}$, where ϕ_{TOE} is the monomer density at the site the other end tries to move in. Likewise, the increase occurs with a probability proportional to $1 - \phi_1$, where ϕ_1 is the monomer density at the site in the first layer next to the chain end. In the absence of the excluded volume, the increase and decrease occur with the same success probability, resulting in the profile given by eq 1 with $m = 2$. With the excluded volume present, the decrease is more difficult because $\phi_{TOE} > \phi_1$. This unequal propagation of the chain segments results in an increase in the monomer density near the walls compared with the scaling prediction that changes the exponent m only. The increase is greater in the semidilute solutions, in the strong confinement, or in Θ solvent as we see in

Table 2. These solutions have a high monomer density at sites next to occupied sites in the middle of the slit. Although we used the reptation moves to explain the incentive, we could also use another type of chain update that moves the segments between layers. For kink jumps on the cubic lattice and bond fluctuation models, for instance, we can develop a similar discussion. We expect that it will be common to different chain update algorithms that uneven space filling in the slit gives an incentive for the segments to be near the wall where the monomer density is lower, but it needs to be proved or disproved. Another test of our hypothesis will be to use simulations on three-dimensional lattices with a coordination number Z other than 6 and on a two-dimensional square lattice. The effect of site occupancy on the successful chain move will depend on Z. It is also necessary to employ off-lattice molecular dynamics simulations to find the universality of the positive γ.

Conclusions

We carried out lattice Monte Carlo simulations for polymer solutions confined to a slit and obtained the monomer density profiles. Results were compared with the predictions of the scaling theory developed for a continuous medium. We found that a positive penetration depth is needed for the scaling theory to describe the density profile of athermal chains in the dilute and semidilute solutions and Θ chains in the two concentration regimes. The penetration depth is 0.36 of the lattice unit when the chains are congested by either a high average concentration or self-association. It was 0.13 for athermal chains at low concentrations. With these corrections, the simulation results agree with the scaling theory. Further studies are needed in other conditions of confinement including different confinement strengths and different geometries of confinement.

References and Notes

(1) Dickman, R.; Hall, C. *J. Chem. Phys.* **1988**, *89*, 3168.
(2) Cifra, P.; Bleha, T.; Romanov, A. *Makromol. Chem., Rapid Commun.* **1988**, *9*, 355.
(3) Yethiraj, A.; Hall, C. K. *J. Chem. Phys.* **1989**, *91*, 4827.
(4) Bleha, T.; Cifra, P.; Karasz, F. E. *Polymer* **1990**, *31*, 1321.
(5) Yethiraj, A.; Hall, C. K. *Mol. Phys.* **1991**, *73*, 503.
(6) Rouault, Y.; Dünweg, B.; Baschnagel, J.; Binder, K. *Polymer* **1996**, *37*, 297.
(7) Thompson, A. P.; Glandt, E. D. *Macromolecules* **1996**, *29*, 4314.
(8) Jorge, A.; Rey, A. *J. Chem. Phys.* **1997**, *106*, 5720.
(9) Wang, Y.; Teraoka, I. *Macromolecules* **1997**, *30*, 8473.
(10) Wang, Y.; Teraoka, I. *Macromolecules* **2000**, *33*, 3478.
(11) Teraoka, I.; Wang, Y. *Macromolecules* **2000**, *33*, 6901.
(12) Cifra, P.; Bleha, T.; Wang, Y.; Teraoka, I. *J. Chem. Phys.* **2000**, *113*, 8313.
(13) Cifra, P.; Bleha, T. *Macromol. Theory Simul.* **2000**, *9*, 555.
(14) Cifra, P.; Bleha, T. *Macromolecules* **2001** *34*, 605.
(15) Cifra, P.; Škrinárová, Z. *Macromol. Theory Simul.*, in press.
(16) de Gennes, P. G. *Scaling Concepts in Polymer Physics*; Cornell University Press: Ithaca, NY, 1979.
(17) Casassa, E. F.; Tagami, Y. *Macromolecules* **1969**, *2*, 14.
(18) Eisenriegler, E. *Phys. Rev. E* **1997**, *55*, 3116.
(19) Shih, W. Y.; Shih, W.-H.; Aksay, I. A. *Macromolecules* **1990**, *23*, 3291.
(20) Dickman, R. *J. Chem. Phys.* **1992**, *96*, 1516.
(21) Milchev, A.; Binder, K. *Eur. Phys. J. B* **1998**, *3*, 477; **2000**, *13*, 607.
(22) De Joannis, J.; Jimenez, J.; Rajagopalan, R.; Bitsanis, I. *Europhys. Lett.* **2000**, *51*, 41.
(23) Panagiotopoulos, A. Z.; Wong, V.; Floriano, M. A. *Macromolecules* **1998**, *31*, 912.
(24) Metropolis, N.; Rosenbluth, A. W.; Rosenbluth, M. N.; Teller, A. H.; Teller, E. *J. Chem. Phys.* **1953**, *21*, 1087.
(25) Teraoka, I. *Prog. Polym. Sci.* **1996**, *21*, 89.
(26) Teraoka, I.; Wang, Y. *J. Chem. Phys.*, in press.
(27) Wiltzius, P.; Haller, H. R.; Cannell, D. S.; Schaefer, D. W. *Phys. Rev. Lett.* **1983**, *51*, 1183.

MA010158J